RECENT TRENDS IN TERTIARY TREATMENT OF WATER/WASTEWATER

Column optimization of adsorption and evaluation of bed parameters-based on removal of arsenite ion using rice husk

Monika Antil[1] · Surinder Singh[2] · Mamta Bhagat[1] · Vishal Vilvas[1] · Suresh Sundaramurthy[3]

Abstract

The objective of this study deals with column optimization of adsorption-based on removal of arsenite ion using rice husk. The parameters affecting the column adsorption study, i.e., influent-concentration, bed depth, and flow rate, were optimized. The range of parameters, i.e., influent-concentration (15–50 mg/L), flow rate (20, 35, 45, and 60 mL/min), and bed depth (15–60 mm), were studied experimentally. Kinetics models Bohart-Adams and Hutchins were studied to measure the amount adsorbed, depth of mass transfer zone, saturated concentration, and time observed at 10% & 90% breakthrough. The percentage amount adsorbed q_m enhanced with enhancement in bed depth but got reduced with influent ions concentration and volumetric flow rate. Established model Bohart-Adams and Hutchins equations were used for calculation of mass transfer zone which came out to be 51 mm. An adsorption capacity (q_m) of 4.5 mg/g for arsenite ions was achieved at optimum parameter values of 60 mm of bed depth, 20 mL/min volumetric flow rate, and 50 mg/L of influent ions concentration. The adsorption bed parameters were also evaluated using Hutchins and Michaels equations. The column study proved rice husk to be a potential adsorbent for the adsorption of arsenite.

Keywords Arsenite · Fixed-bed column · Breakthrough curve · Adsorbent · BDST model · Hutchins model

Introduction

Arsenic is a metalloid and has other allotropes and forms. It has different applications in electronics, agriculture, wood preservatives, medicine and metallurgy. It is used in car batteries, ammunition, production of pesticides, herbicides, insecticides, and treated wood products (Nicomel et al. 2015). No doubt, arsenic has different uses in different fields (Shen, 1997), but due to its toxicity, its applications are declining (Fig. 1).

Most research studies have been published on the equilibrium study to remove metal ions using the adsorption process (Pholosi et al. 2020). A limited volume of adsorbate can be treated using the equilibrium method, i.e., batch study, while a wide range of adsorbate can be utilized in the dynamic study (Ahmad and Hameed 2010).The different techniques available for separation of ions from aqueous solution include advanced oxidation (Kurian 2021; Zaw and Emett 2002), electrochemical separation (Gilhotra et al. 2021), coagulation- flocculation (Francisca and Carro Pérez 2014; Han et al. 2002), reverse osmosis (Arslana, et al. 2011),nanofiltration (Maher et al. 2014; Noel et al. 2021) etc. These have been commonly utilized for abatement of arsenite and other heavy metal ions from aqueous or synthetic solutions (Nurul et al.2006). Adsorption (Yu et al. 2021; Jung et al. 2019; Shipley et al. 2009; Mohan et al. 2019; Golberg 2002) is the most widely used technique in water pollution abatement (Sahin et al. 2021; Kutluay et al. 2020a, b) due to its operational flexibilities, availability of low-cost effective adsorbents, and its simplicity. Various adsorbents such as coal derived char (Batur et al., 2021), modified peanut shell Kutluay et al. 2020a, b), oxide-coated natural materials (Asere et al. 2019; Maji et al.

✉ Surinder Singh
sonuunos@gmail.com

1 Deenbandhu Chhotu Ram University of Science & Technology, Murthal, 131039 Sonipat, India

2 Dr. S. S. Bhatnagar University Institute of Chemical Engineering and Technology, Panjab University, Chandigarh, India

3 Department of Chemical Engineering, Maulana Azad National Institute of Technology , Bhopal 462 003, Madhya Pradesh, India
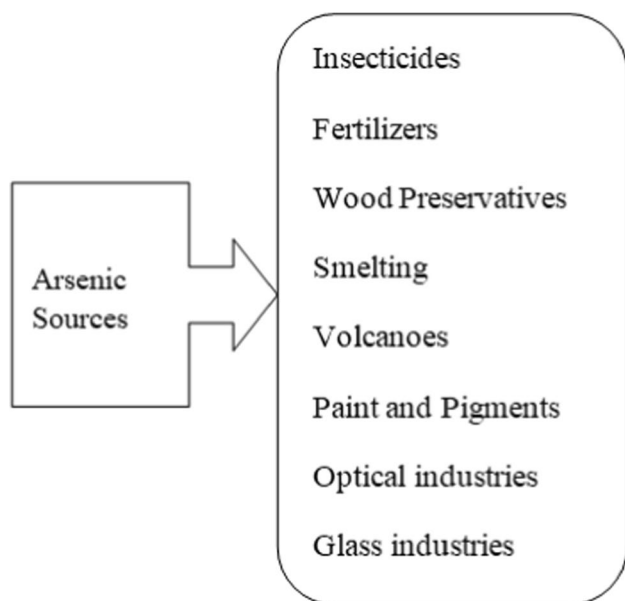
Fig. 1 Sources of arsenic

Fig. 2 Properties of rice husk

2012; Siddiqui and Chaudhry 2017), laterite soil (Maji et al. 2008), sludge (Byambaa et al. 2021), carbon-based adsorbents (Islam et al. 2021; Chen et al. 2007), waste by-products (Mukherjee et al. 2021; Senthilkumar et al. 2020), biochar (Liu et al. 2012; Lin et al. 2017), nanocomposites (Siddiqa et al. 2019), Fe(III) loaded cotton cellulose (Zhao et al. 2009), and sirnak coal-derived char (Batur et al. 2021) have been utilized by different researchers. Few researchers have used different activating agents like KOH (Islam et al. 2017), H_3PO_4 (Abatan et al. 2019; Baytar et al. 2021), and NaOH (Giri et al. 2020) for adsorbents for different bio adsorbents. This study focused on agriculture waste, i.e., rice husk (RH) to remove arsenite ions using dynamic or column study. Raw rice husk can be utilized as an adsorbent to remove arsenic as a potential adsorbent (Nurul et al. 2006; Asif and Chen 2017). In 2019–20 "The United States Department of Agriculture" estimated 496.22 million metric tons of rice production in the World. About 20% of the entire rice grain mass is rice husk. Few properties of rice husk are shown in Fig. 2 (Kalderis et al. 2014).

Several researchers have examined the potential of modified and unmodified rice husk to be used as an adsorbent in equilibrium and dynamic mode for abatement of heavy metal contaminants from wastewater (Ahmaruzzaman 2011; Dang et al. 2009). Dang et al. (2009) reported the adsorption capacity (2.24 mg/g) of iron-modified RH for abatement of arsenic ions using batch mode. The arsenic ions adsorption by RH-Fe was affected by pH and other parameters. Pehlivan et al. (2013) observed the adsorptive removal of As(V) ions on Fe (III)-coated RH in batch mode using various parameters such as pH, As(V) concentration, contact time, ionic
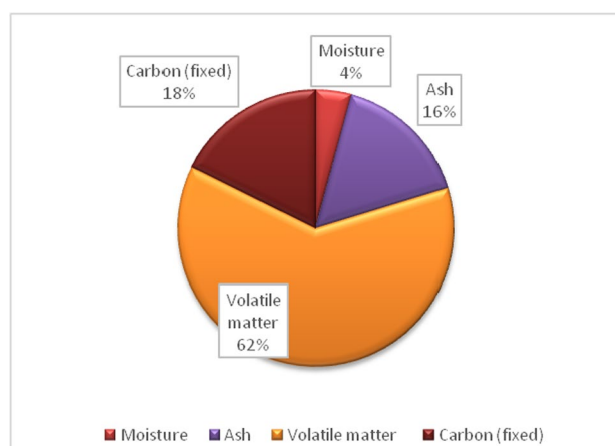
strength, and adsorbent amount. At pH 4, maximal removal of As(V) ions was 94% and adsorption capacity obtained was 2.5 mg/g. Mostly the adsorption was carried out using batch adsorption. As very few studies have been conducted for the removal of As ions using fixed bed column. A few of these studies only reported calculated adsorption capacity/percent removal of rice husk, but none has determined the different adsorption zone parameters for the fixed bed columns. Some recent studies have incorporated magnetic nanoparticles for removal of volatile organic compounds like benzene and toluene and reported their adsorption–desorption and recyclability studies (Ece et al. 2020; Sahin et al. 2021). The recyclability studies help in ascertaining the use of adsorbent for repeated cycles and its improving its efficiency. The studies utilized for adsorption of arsenite and other ions using rice husk are summarized in Table 1. The present study deals with the calculation of different column bed design factors such as the time taken for adsorptive zone to move its depth down the column, total time taken by adsorptive zone to form, height of the adsorptive zone, percentage bed saturation etc. which are not reported in the literature. The results show that waste rice husk is a potent sorbent for removal of arsenite ions from wastewater using dynamic mode and these mathematical models can be implemented for the designing of the adsorption column.

The prime aim of research study was optimization of column adsorption, based on removal of arsenite ion using rice husk.

Materials utilized and methods

Adsorbate and reagents

All the materials (chemicals) utilized in this research were of analytical grade (AR). The standard solution of arsenite ions

Table 1 Studies reported in literature on removal of different metal-ions from water and/or wastewater using RH

S. No	Adsorbate	Parameters studied	Mode of experiment	Models studied	Results (removal %/amount adsorbed)	Reference
1	As(V) from drinking water	Adsorbent = Rice Husk, Dose of adsorbent = 42.5 g, vol. flow rate = 7 mL/min, column diameter = 5 cm, bed height = 28 cm inlet feed concentration = 15 ppb	Column adsorption	BDST model, Yoon-Nelson, Thomas Model	Removal 90.70%	Asif and Chen(2017)
2	As(III) and As(V) ions	Adsorbent = Thioglycoalated sugarcane carbon, Adsorbent dose- 6.0 g, vol. flow rate 3.0 mL/min, and initial As ions concentration 1,500 mg/L	Batch and column	Thomas model	85.01 µg/g As(V) for As(III) and 83.82 µg/g As(V)	Roy et al. 2013
3	As ions	Biochars (activated and non-activated) made from sawdust and rice husk, Temperatures used (300 and 700 °C)	Column leaching experiments	–	Leaching into groundwater prevented utilizing biochar	Amin et al. 2020
4	Arsenite	Modified RH at 150°C, unmodified RH also used	Batch	–	Removal efficiency, 75.00%	Samad et al. 2016
5	Arsenite	Adsorbent = Rice Husk, Parameters: 180 min, pH value of 7–8	Batch	Kinetic model–pseudo second-order Adsorption-isotherms, Freundlich and Langmuir	adsorption capacity, 1.897 mg/g	Khan et al. 2012
6	As(V)	Adsorbent = Macromolecule carbonized Rice Husk, Initial adsorbed concentration (10–100 µg/L), contact time (3–90 min), adsorbent dose (0.5–6 g/l) and pH (3–9)	Batch	–	Removal efficiency of As increased up to 85.00%	Babazad et al. 2021
7	As(III) & As(V)	Adsorbent = Rice Husk, At pH 7, maximum adsorption capacities were 19.1 and 20.3 mg/g, respectively	Batch	Langmuir and Freundlich non-linear isotherm models (R2 > 0.98)	The FMRS (q_e = 11.9 mg/g) and original rice husk ash (q_e = 0.4 mg/g) at initial [As(V)] = 5 mg/L	Batur et al. 2021
8	Tetracyclie antibiotics	Activated Carbon, mass ratio of zinc chloride, rice husk carbon (RHC), activation temperature and contact time	–	–	(R^2) values 0.9955 to 0.9998. LOD and LOQ (quantization) were 0.10 to 0.95 and 0.35 to 2.85 mg L^{-1} respectively	Louet al. 2016

Table 1 (continued)

S. No	Adsorbate	Parameters studied	Mode of experiment	Models studied	Results (removal %/amount adsorbed)	Reference
9	Sodium-ion	Adsorbent = Wheat straw, pH (4.3 to 8), contact time (10–180 min), Adsorbent dosage (0.3–1.6 g) and the initial concentration (5–120 mg/L)	Batch	Elovich model, Langmuir and Freundlich non-linear isotherm models	Adsorption efficiency ranged from 85.49 to 68.07% for wheat straw (WH) and 89.43 to 68.20%. for RH Max ads cap was 9.43 mg/g	Rasouli et al. 2020
10	Fe(III) and Mn(II)	Adsorbent = Rice Husk carbon	Batch	Langmuir and Freundlich adsorption isotherms	RH as activated carbon gave better results	Masoud et al. 2016
11	Ni, Zn, Cd, Mn, Co, Cu, Hg and Pb	Initial adsorbed concentration 50–200 mg/L, Contact time (3–90 min) and pH (5.5–6)	Batch and column	Langmuir and Freundlich adsorption isotherms	Maximum adsorption capacity obtained from the Langmuir isotherm (mmol/g): Ni = 0.094 Zn = 0.124 Cd = 0.149 Mn = 0.151 Co = 0.162 Cu = 0.172 Hg = 0.180 Pb = 0.280	Krishnani et al. 2008
12	Cr(VI)	Initial adsorbed concentration (10–250 mg/L), contact time (60–120 min) and pH 5.2	Batch	Langmuir, Freundlich, Temkin, Dubinin–Redushkevich adsorption isotherms	Maximum adsorption = 78.60% at pH 5.2	Khalil et al. 2021

was made by dissolving 0.132 g of arsenic trioxide salt in 1L deionized water (DI). Then, this solution was mixed and prepared well and stored in the dark. The aqueous solution of different concentrations of arsenite ions was prepared using this stock solution. All chemicals used in this investigation were of the analytical standard of purity. Alkaline chemical 'sodium-hydroxide' and acidic chemical 'hydrochloric acid' were used to set the pH values of the samples.

Rice husk as an adsorbent

Rice husk was taken from Kohinoor Foods Ltd., Murthal, Sonepat, India. It was then cleaned thoroughly with deionized water to separate impurities like dust particles and followed drying for 24 h at 100 °C in an oven (El-Shafey 2007).

Dynamic study

A Borosil make glass column having an inner diameter of 30 mm and an altitude of 720 mm was utilized for the different experiments in this study. The column was fixed vertically as shown in Fig. 3 (Ayoob et al. 2007) and the arsenite ion solution was delivered through the delivery line from the storage tank to the column. Inside the column, 0.4 mm of the screen was adjusted at bottom and top to support the adsorbent media (Jain et al., 2013).

The effect of the bed depth of rice husk, the flow rate of arsenite ion solution, and influent concentration were studied. The color intensity of arsenite is directly proportional to its concentration. By varying the concentration of arsenite solution calibration curve was constructed and its absorbance was measured at $\lambda_{max} = 194$ nm by using a UV–Visible spectrophotometer (RIGOL Ultra-3660) (Ayoob et al. 2007; Shahlae and Pourhossein 2014).

Results and discussion

Effect of bed depth

The adsorption capacity of rice husk was observed by varying the bed depth 15, 30, 45, and 60 mm (Mohan et al. 2017; Dotto et al. 2015; Song et al. 2016, Fallah and Taghizadeh 2020). The breakthrough curve was obtained by keeping the arsenite ions concentration constant at 50 mg/L and 20 mL/min of flow rate (FR) in 30 mm of inner and 32 mm outer diameter column. In Fig. 4 (a), it was observed that the breakthrough time at 10% effluent concentrations increased on increasing the bed depth (Golie and Upadhyayula 2016; Singh and Pant 2006; Hummadi et al. 2022) as there is an increase in the surface area of the adsorbent bed on increasing the bed depth. The breakthrough time at 10% effluent concentration ($t_b 10\%$) increased from 7 to 20 min on increasing the bed depth from 15 to 60 mm. Hence, the optimum bed depth was found out to be 60 mm.

Influence of different flow rates

The analysis was done at different flow rates of 20, 35, 45, and 60 mL/min (Mohan et al. 2017; Dotto et al. 2015; Song et al.2016, Fallah and Taghizadeh 2020; Hummadi et al. 2022). As shown in Fig. 4 (b), the breakthrough curves obtained at different flow rates were observed, keeping the concentration of arsenite at 50 mg/L and bed depth at 60 mm. The breakthrough time decreases on increasing the flow rate (Golie and Upadhyayula 2016; Singh and Pant 2006; Fallah and Taghizadeh 2020). The breakthrough time at 10% effluent concentrations ($t_b 10\%$) decreased from 20 to 6 min by increasing the flow rate from 20 mL/min to 60 mL/min [Fig. 4(b)]. At lower flow rate, the adsorbate is in contact with the adsorbent for a longer time and results in higher adsorption. In other words, at lower flow-rate, adsorbate pass slowly through the column and takes much time to achieve saturation whereas higher flow-rate, adsorbate gets lesser time to get adsorbed on to the surface of adsorbent, i.e., the residence time of the adsorbate decreased; hence, removal of arsenite ions decreased with increasing flow-rates (Asif and Chen2017). Hence, flow rate of 20 mL/min was adjudged to be the optimum flow rate.
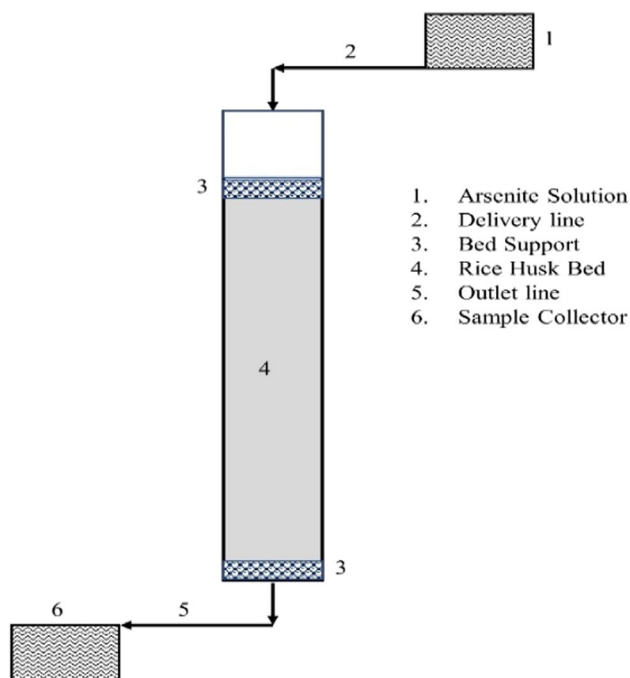

Fig. 3 Experimental setup of dynamic study

1. Arsenite Solution
2. Delivery line
3. Bed Support
4. Rice Husk Bed
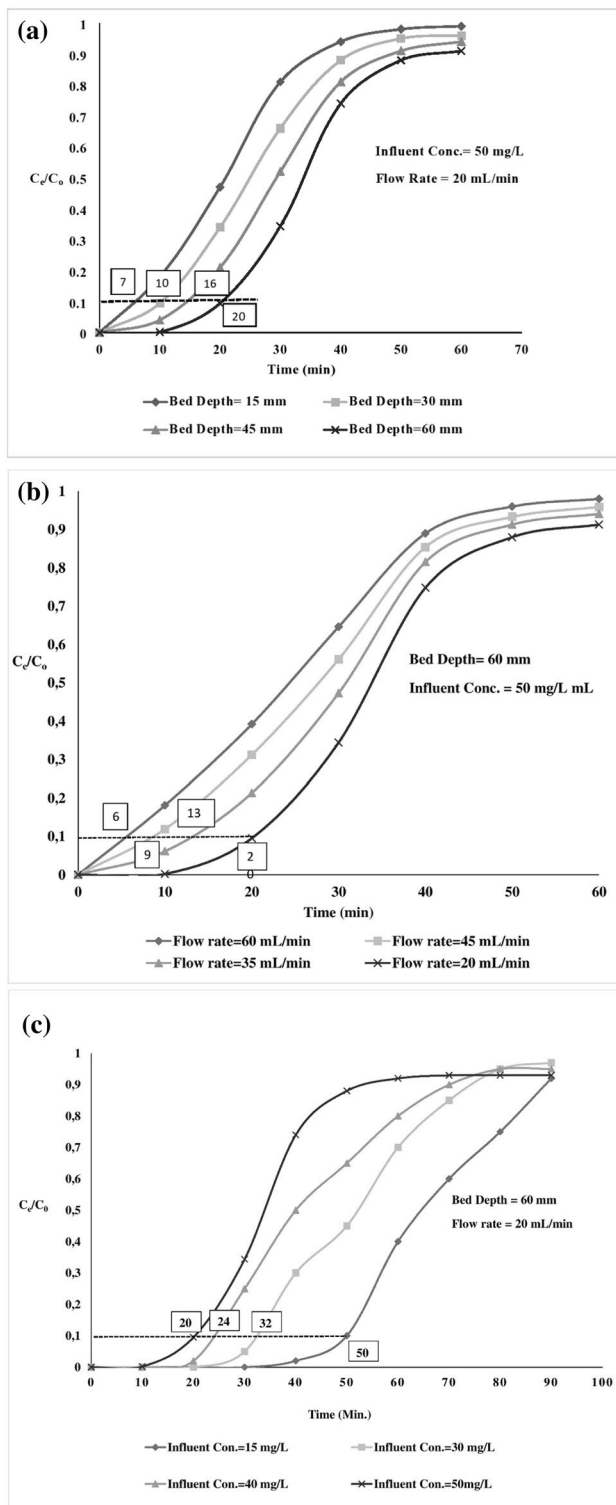5. Outlet line
6. Sample Collector

Fig. 4 (a) Breakthrough curves at different bed depths of rice husk. (b). Breakthrough curves at the different flow rates of arsenite ion. (c) Influence of influent concentration of arsenite ions on the breakthrough curves

Influence of different arsenite ion concentrations

The adsorption efficiency of rice husk was also investigated with varying influent concentrations in the range of 15–50 mg/L (Mohan et al. 2017; Dotto et al. 2015; Song et al. 2016, Fallah and Taghizadeh 2020). The behavior of the breakthrough curve was studied by keeping the bed depth at 60 mm and 20 mL/min of flow rate in the column. As shown in Fig. 4 (c), the breakthrough time (at 10% effluent concentration) decreased (from 50 to 20 min), with increasing the influent concentration from 15 to 50 mg/L. It can be attributed to the fact that on increasing the influent concentration, there is an increase in the number of arsenite ions to be adsorbed but the number of adsorption sites available on the surface of the adsorbent remains same as the bed depth was kept constant for these experiments. Hence, the amount of adsorbed ions decreased with increased influent concentration of arsenite ions (Liao et al. 2013; Fallah and Taghizadeh 2020; Singh and Pant 2006; Hummadi et al. 2022).

Bohart-Adams model

The Bohart-Adams model is applied to find depth of mass transfer zone. This kinetic model depends upon the surface reaction rate. Therefore according to this model, the service time was calculated by using the equation.

$$\ln\left(\frac{C_o}{C_e} - 1\right) = \ln\left(e^{kN_o\frac{x}{v}} - 1\right) - kC_o t \tag{1}$$

Since the exponential term, $e^{\frac{kNo}{v}} >> 1$; hence, unity term was neglected. Then, the equation becomes

$$\ln\left(\frac{C_o}{C_e} - 1\right) = \ln e^{kN_o\frac{x}{v}} - kC_o t \tag{2}$$

where:

C_o & C_e are the influent and effluent concentration in mg/L

x: bed height in mm

k: adsorption rate constant in mL/mg$^/$min

N_o: indicate amount adsorbed (mg/cm^3)

v: linear flow velocity of the influent into the column(mL/min/cm^2)

and t is the service time in min (Pholosi et al. 2020; Goyal et al. 2009; Yan et al. 2001)

Since,

$$\ln e^{kN_o\frac{x}{v}} = kN_o\frac{x}{v} \tag{3}$$

We have

$$\ln\left(\frac{C_o}{C_e} - 1\right) = kN_o\frac{x}{v} - kC_o t \tag{4}$$

Which is the same as

$$(v)\ln\left(\frac{C_o}{C_e} - 1\right) = kN_ox - kC_ot\,(v) \tag{5}$$

Multiplying both sides by $\frac{N_o}{N_o}$ and dividing both sides by kN_o yields

$$\frac{v}{kN_o}\ln\left(\frac{C_o}{C_e} - 1\right) = x - \frac{vC_ot}{N_o} \tag{6}$$

Which can be solved for t

$$t = \frac{N_o}{C_ov}x - \frac{1}{C_ok}\ln\left(\frac{C_o}{C_e} - 1\right) \tag{7}$$

the N_0, C_0 and k, values can be calculated from column experiments, which operated with linear velocity values (Goyal et al. 2009; Baral et al. 2009; Ahmad and Hameed 2010; Abdolali et al. 2017; Zhang et al. 2017).

Hutchins (Hutchins 1973) proposed changes in the Bohart-Adams model equation, which only requires three fixed-bed column runs to acquire the required essential data. The procedure was termed as "bed depth service time" (BDST) model. The Bohart-Adams model Eq. (7) can be depicted in linear form as follows.

$$t = ax + b \tag{8}$$

$$\text{Slope}\,a = \frac{N_o}{C_oV} = 0.4 \tag{9}$$

$$\text{Intercept}\,b = \frac{1}{kC_o}\ln\left(\frac{C_o}{C_e} - 1\right) = -1.5 \tag{10}$$

as shown in Fig. 5 (a).

If the time value is zero, Eq. (7) reduces to:

$$x_0 = \frac{V}{KN_0}\ln\frac{C_0}{C_e} \tag{11}$$

x_0 = minimum/critical adsorbent bed depth, at which effluent concentration passes through it and Adsorption Zone/Mass Transfer Zone Depth = 51 mm as shown in Fig. 5 (b). These results obtained were in agreement with the literature available on calculated parameters using the Bohart-Adams model (Table 2) (Marzbali and Esmaieli 2017; Charola et al. 2018; Chowdhury et al. 2015; Patel and Vashi 2015).

At different values of flow rate, an effective adsorbed amount was obtained using breakthrough time (t_b) at 10% breakthrough concentration (saturated) using the following equation:
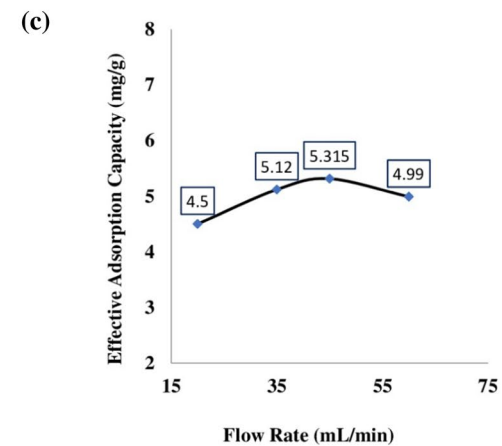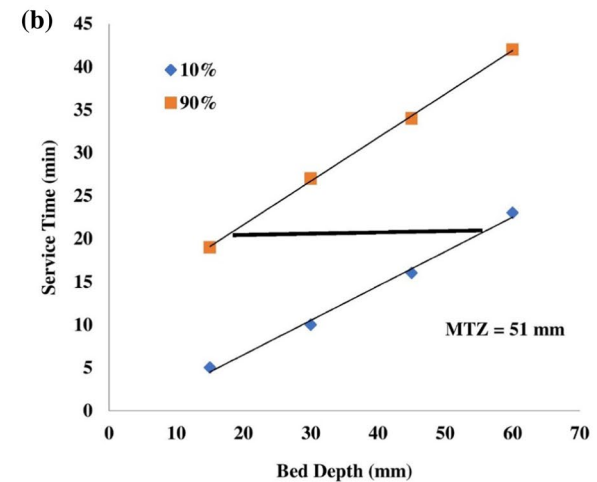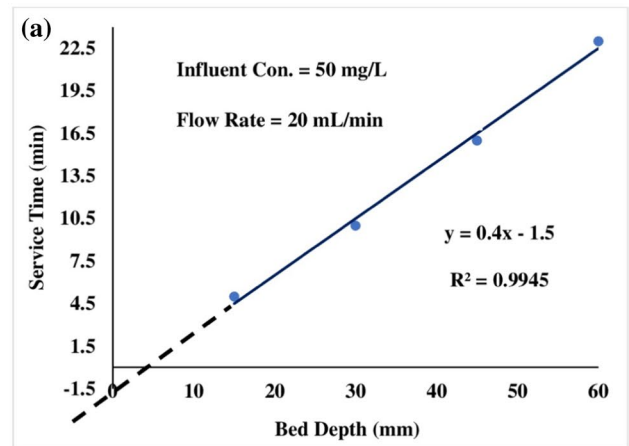

Fig. 5 (**a**) BDST plot for arsenite ions at a flow rate for 10% breakthrough concentration. (**b**) BDST plot at two different effluent concentrations arsenite ions. (**c**) Influence of volumetric flow rate on adsorption capacity of adsorbent

$$\text{Effective amount adsorbed}\,(q_e) = \frac{t_b.Q.(C_0 - C_e)}{w} \tag{12}$$

where:

Q: flow- rate (mL/min).

Table 2 Bohart-Adams parameters at particular flow-rate using BDST plots

Adsorbent	Flow rate (mL/min)	Slope (min/mm)	Intercept (min)	V (mL/mm)	K (mLmg^{-1} min^{-1})	N$_o$ (mg/mm^3)	Critical bed depth x$_0$ (mm)	
							Using Eq. (11)	From Figure 5 (a)
Rice Husk	20.00	0.40	−1.500	0.0295	0.029	0.0059	3.788	4.000

C_0 and C_e: the inlet and outlet concentration in mg/L.

w: represents weight of Rice Husk (g) in column.

q_e: is an amount of arsenite ions adsorbed.

Figure 5 (c) shows a plot of the amount adsorbed at 10% effluent against the flow rate. The adsorption increases gradually with flow rate, but tends to become slower at a higher flow rate due to mass transfer effect. In the fixed-bed column, maximum adsorption capacity (q_m) 5.315 mg/g occurred at 45 mL/min flow rate as shown in Fig. 5 (c).

Adsorption column design parameters

Hutchins (Hutchins 1973) recommended to use column design parameters of one experiment to calculate parameters at other concentration values and flow rates. As per BDST model, the value of a* can be obtained at any feed concentration as well flow rate by the equation given as follows (Han et al. 2008; Srivastava et al. 2008; McKay 1979).

$$a^* = a\frac{Q_1}{Q_2} \qquad (13)$$

$$As; t = ax + b \qquad (14)$$

$$For t^* = a^*x + b \qquad (15)$$

Similarly, for influent concentration

$$a^* = a\frac{C_1}{C_2} \qquad (16)$$

$$b^* = b\left(\frac{C_1}{C_2}\right)\frac{\ln(\frac{C_2}{C_F} - 1)}{\ln(\frac{C_2}{C_B} - 1)} \qquad (17)$$

$$t^* = a^*x + b^* \qquad (18)$$

t_b values, i.e., experimental run values and those obtained using Eq. (18) at different feed concentrations are enlisted in Table 3. The experimental and calculated values are quite comparable.

Table 3 t_b values, i.e., experimental run values and those obtained using Eq. (18) for different feed concentrations. Bed depth = 60 mm. Flow rate = 20 mL/min

Feed Conc. = 30 mg/L		Feed Conc. = 40 mg/L		Feed Conc. = 50 mg/L	
t_b (min) (experimental)	t_b (min) (cal. from Eq. (18))	t_b (min) (experimental)	t_b (min) (cal. from Eq. (18))	t_b (min) (experimental)	t_b (min) (cal. from Eq. (18))
34.0	28.5	32.0	27.0	20.0.0	22.5

Table 4 Adsorption zone parameters for the column. Flow rate = 20 mL/min. Feed concentration = 50 mg/L

Adsorptive zone parameters	Bed depth (60 mm)	Bed depth (45 mm)	Bed depth (30 mm)	Bed depth (15 mm)	Average values
t_z (min)	19.00	18.00	17.00	14.00	17.00
h_z (mm)	28.43	25.15	20.16	11.93	21.42
V_z (mm/min)	1.496	1.397	1.186	0.852	1.233
Bed saturation (%)	95.26	94.4	93.28	92.05	93.75

The parameters were evaluated using the method of Michaels, Mass Transfer Operations (textbook) by Treybal, R.E., (1981)

Column adsorption zone parameters

Adsorption zone formation and dynamics have been calculated (Table 4) using the rice husk column data obtained in this study using Eqs. (19)–(25).

$$t_z = \frac{V_Z}{Q_f} = \frac{V_E - V_B}{Q_f} \qquad (19)$$

where:

t_z: represents time required for adsorptive zone to move its depth down the column after becoming established

V_z: represents actual volume of inlet aqueous solution used in between the break through point and exhaust point

V_E: represents volume of aqueous solution to exhaust point whereas V_B represents volume of aqueous solution to breakthrough point (mL)

Q_f: depicts solution flow rate (mL/min)

Also, t_E represents time needed for the adsorptive zone to become fully confirmed and traverse fully out of the adsorptive bed, expressed by following equation;

$$t_E = \frac{V_E}{Q_f} \tag{20}$$

Movement rate of adsorptive zone down the bed is expressed as;

$$V_z = \frac{h_z}{t_z} = \frac{x}{t_E - t_o} \tag{21}$$

where h_z represents adsorptive zone height (mm), x represents bed depth (mm), t_F depicts time needed for adsorptive zone to form initially (min) so that,

$$h_z = \frac{x t_z}{t_E - t_F} \tag{22}$$

The value of t_F cannot be measured directly but ascertained mathematically using Michaels' method as given by the following equation:

$$t_F = (1 - F)t_z \tag{23}$$

where F represents fraction of RH available in adsorptive zone.

$$F = \frac{S_z}{S_m} = \frac{\int_{V_E}^{V_z}(C_o - C)dv}{C_0(V_E - V_B)} \tag{24}$$

S_z: depicts amount of solute separated by adsorptive zone between breakthrough point to exhaustive point

S_m: represents solute withdrawn by adsorptive zone at exhaustion point.

F value or amount was utilized to obtain percentage saturation of adsorptive column, as follows:

$$\%Saturation = \frac{x + (1 - F)h_z}{h} \times 100 \tag{25}$$

Characterization of rice husk

Fourier-transform infrared spectroscopy

FTIR spectroscopy is an effective method used to identify the characteristic functional groups present on the adsorbent surface. FTIR analysis of natural rice husk before and after adsorption was carried out and has been shown in Figs. 6 and 7. The adsorption peak at 3434.6 and 3417.3 cm^{-1} referred to the presence of free –OH groups. The CH stretching height around 2925.2, 2923.4, 2856.2, and 2854.5 cm^{-1} attributes to the presence of a carboxylic acid group. The peak at 2063.0 and 2060.9 cm^{-1} indicates the alkynes group. The peaks around 1634.5–1636.8 cm^{-1} correspond to the CO group. Alkenes and aromatic functional groups are shown by the C=C stretching vibrations from range 1546.80–1652.88 cm^{-1}. The presence of CH_2 and CH_3 groups indicates at the peak of wave number 1458.0 cm^{-1} while at wave number 1380 cm^{-1} indicative of CH_3. Rice husk at 1374.4–1384.3 cm^{-1} referred to the aromatic hydrocarbon CH group. The peak range of 1100–1250 cm^{-1} indicates the alcohol CO group. The peaks range of 400–600 cm^{-1} means alkyl halides (Bansal et al. 2009; Daffalla et al. 2012; Deshmukh et al. 2012). Table 5 gives the summary of functional groups present in the FTIR spectra.
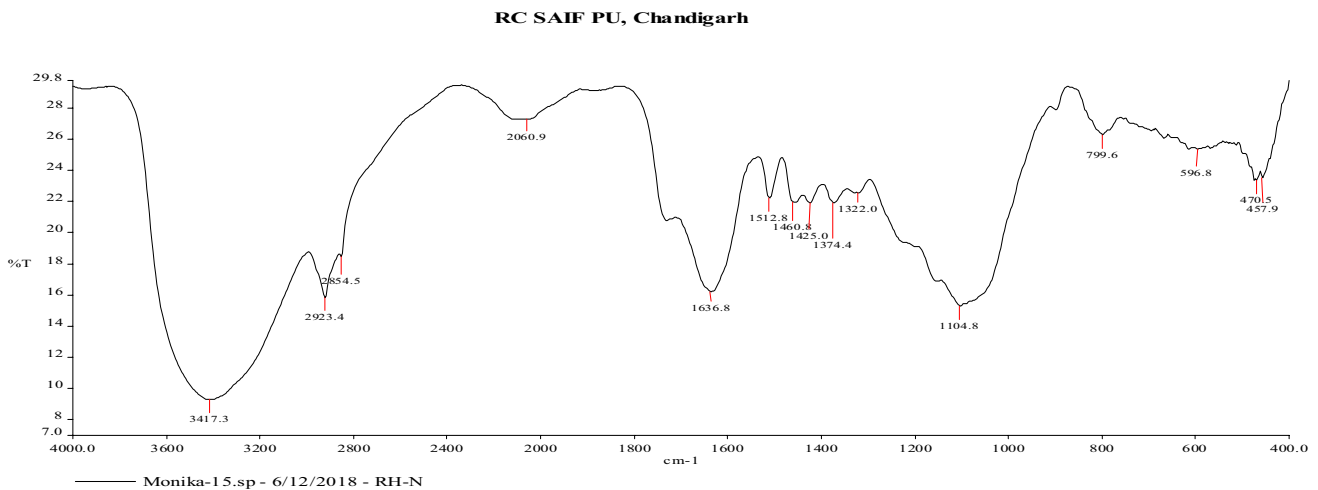

RC SAIF PU, Chandigarh

Monika-15.sp - 6/12/2018 - RH-N

Fig. 6 FTIR spectra of rice husk before adsorption
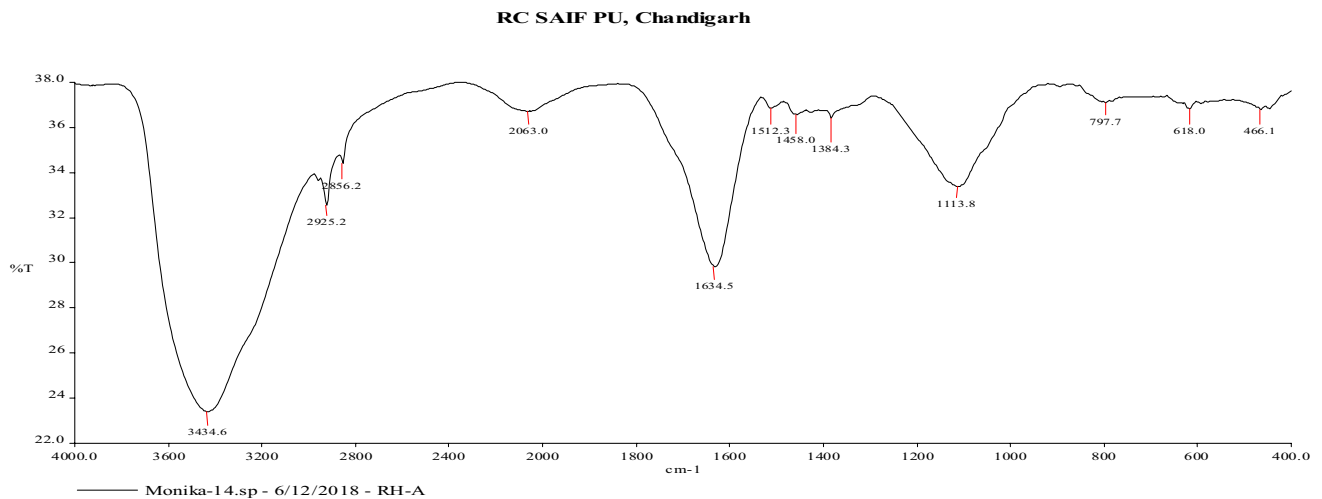
RC SAIF PU, Chandigarh

Fig. 7 FTIR spectra of rice husk after adsorption

Table 5 FTIR spectra of rice husk before and after adsorption

Adsorption peak range/wave number	Major chemical group
3434.6 cm^{-1}	Si–OH groups, hydroxyl group -OH
3417.3 cm^{-1}	Hydroxyl group –OH, Si–OH
2925.2, 2923.4, 2856.2, and 2854.5 cm^{-1}	Carboxylic acid
2063.0 and 2060.9 cm^{-1}	Alkynes group
1634.5–1636.8 cm^{-1}	CO groups
1546.80–1652.88 cm^{-1}	Alkenes and aromatics groups
1458.0 cm^{-1}	CH$_2$, and CH$_3$
1380 cm^{-1}	CH$_3$ groups
1374.4–1384.3 cm^{-1}	CH groups
1100–1250 cm^{-1}	Silicon dioxide SiO$_2$
799 cm^{-1}	Asymmetric and symmetric stretching mode at Si–O-Si
400–600 cm^{-1}	Halides group

XRD characterization

In Fig. 8, the XRD image of raw rice husk is shown. The XRD image of rice husk exhibited broadband at $2\theta = 21.68°\sim22°$ (approximately), which indicated the characteristic peak of amorphous silica. A small peak observed at $2\theta = 28°$ stated the presence of carbon. The XRD image analyses of rice husk indicated the unstructured nature (amorphous) of Rice Husk (Liu et al. 2014; Mohamed et al. 2015).

Scanning electron microscopy

Rice husk has good adsorption capacity due to the presence of silicon dioxide (SiO$_2$). To analyze the surface of rice husk or adsorption power, the scanning electron microscopy technique was used. Scanning electron microscopy
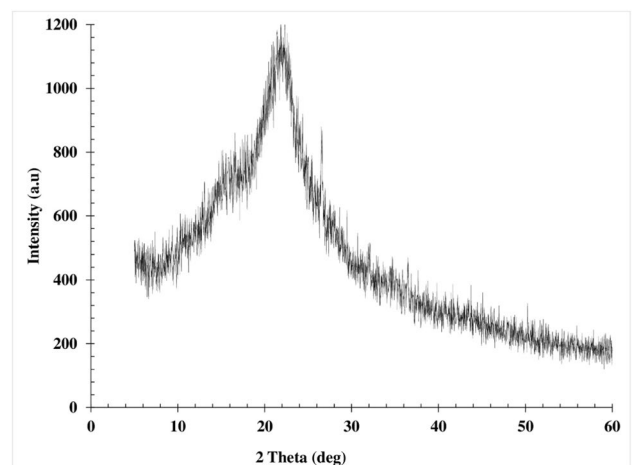

Fig. 8 XRD image of rice husk

images provide the clear morphology of the rice husk, the structure of the surface. In scanning electron microscopy, a focused beam of electrons was used to produce complex, high-magnification images of a rice husk's surface topography. According to the scanning electron microscopy (SEM) micrograph of rice husk, the morphological characteristics of the rice husk structure are spherical in size with irregular geometry in the form of agglomerates in micron-scale operating at 10 kV and at different micron size in Fig. 9. In addition, the uneven, rough, and highly porous structure indicated more surface area (Ahiduzzaman and Islam 2016). Figure 9 illustrates the morphology of the outer surfaces of RH, which is uneven and highly roughened. Silica was found out to be the main inorganic component of RH existing in nanoparticle form. The nano-scale roughness comes from the morphology of silica nanoparticles dispersed within the bulk (Askaruly et al. 2020).

Transmission electron microscopy

For further modification, transmission electron-based microscopy was used. Size and shape of SiO_2 acquired from RH were analyzed using transmission electron microscopy (TEM); the TEM graph and images of size distribution (50–500 μm) of SiO_2 are mentioned in Fig. 10. From the image, it can be identified the spherical SiO_2 (silica)

particles formed the clusters. Particle size of silicon was measured from 500 to 50 μm (Nguyen et al. 2017). As per the TEM images, the rice husk structure is irregular and amorphous in nature.

Conclusions

The experimental study of fixed bed column using rice husk is an appropriate and suitable approach for arsenite ions removal from synthetic wastewater owing to its simplicity, ease in operation, and maintenance. As per this study, the breakthrough time increases on increasing bed depth but decreases on increasing initial concentration and flow rate. The different column design parameters were calculated using the Bohart-Adams theoretical approach and Hutchins equation. The critical bed depth (4 mm) and depth of mass transfer zone calculated using the Bohart-Adams equation agreed closely with the experimental and literature values respectively. The optimized parameters obtained for column study were 60 mm of bed depth, 20 mL/min flow rate, and 50 mg/L of influent-concentration. The t_b value of 20 min at optimized feed concentration (50 mg/L) also matched closely with the value calculated using the Hutchins equation (Table 3). The maximum adsorption capacity obtained at optimized parameters was
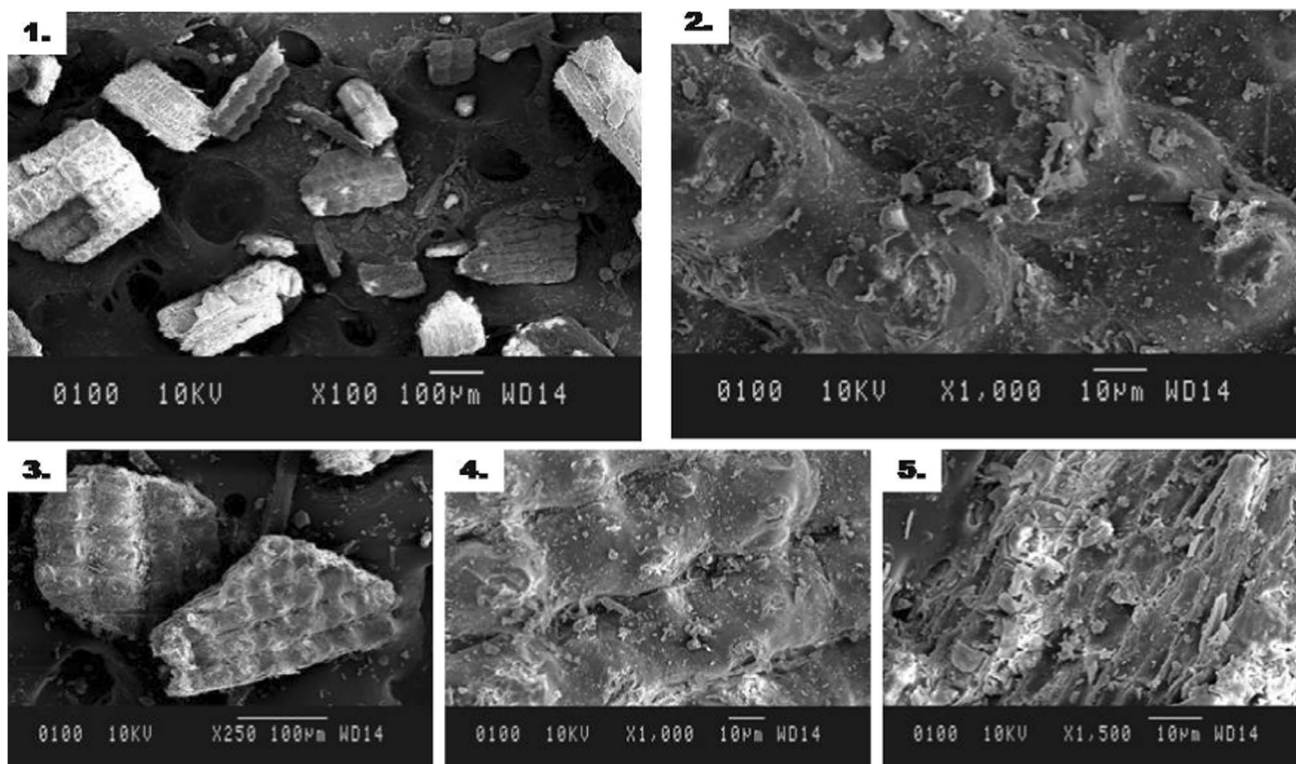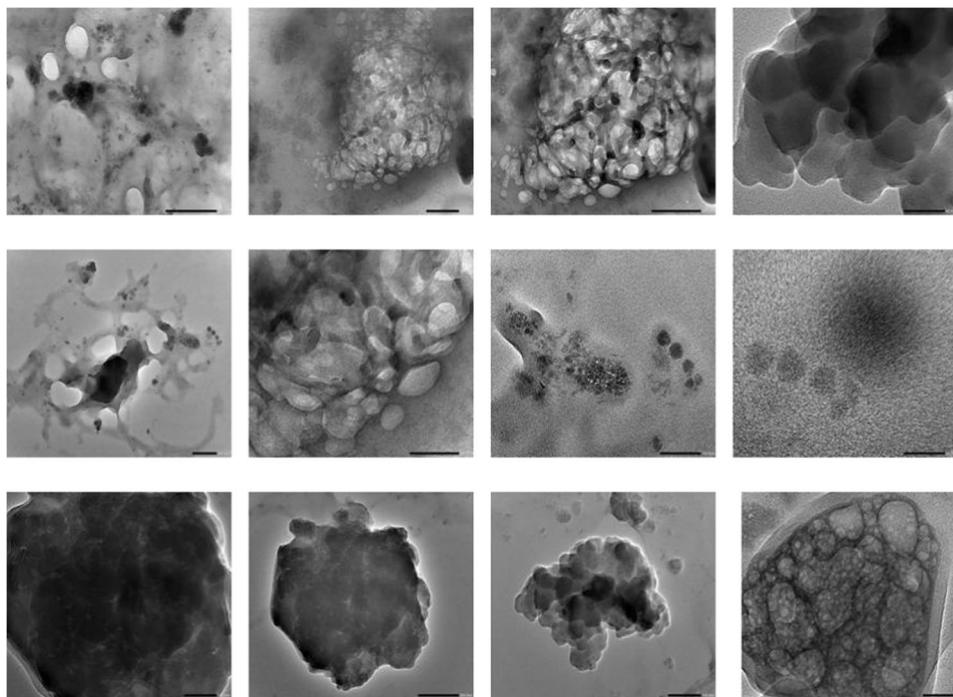

Fig. 9 SEM images of raw rice husk (RRH)

Fig. 10 TEM images of raw rice husk (RRH)

(q_m) 4.5 mg/g. The adsorption zone parameters were also evaluated using Michaels' equations including % bed saturation, time required for the adsorptive zone to become fully established (t_z), and adsorptive bed height (h_z) and were found out to be 95.26%, 19 min, and 28.43 mm at optimized conditions. Hence, column study to separate arsenite ions utilizing rice husk was found to be a potential and efficient method. The future research will need to focus on recycling of heavy metals and eco-friendly waste management of used adsorbents.

Declarations

Ethics approval and consent to participate There are no human participants, animals or client owned animals, human data, or human tissue involved in this study; hence, no ethics approval and consent of any participant or client was required. The general ethics regarding writing of manuscript and data generated and used in the study are however followed.

Consent for publication There is no data in any form (including any individual details, images, or videos) of any individual author or publication/journal or its publisher used in this manuscript or whose permission is required. All the figures and images used are made (belong to)/by the authors of this work.

Competing interests The authors declare no competing interests.

References

Abatan OG et al (2019) Production of activated carbon from African star apple seed husks, oil seed and whole seed for wastewater treatment. J Clean Prod 232:441–450. https://doi.org/10.1016/j.jclepro.2019.05.378

Abdolali A, Ngo HH, Guo W et al (2017) Application of a breakthrough biosorbent for removing heavy metals from synthetic and real wastewaters in a lab-scale continuous fixed-bed column. Biores Technol 229:78–87. https://doi.org/10.1016/j.biortech.2017.01.016

Ahiduzzaman M, Islam AKMS (2016) Preparation of porous bio-char and activated carbon from rice husk by leaching ash and chemical activation. Ahiduzzaman and Sadrul Islam SpringerPlus 5:1248. https://doi.org/10.1186/s40064-016-2932-8

Ahmad AA, Hameed BH (2010) Fixed-bed adsorption of reactive azo dye onto granular activated carbon prepared from waste.

J Hazard Mater 175(1–3):298–303. https://doi.org/10.1016/j.jhazmat.2009.10.003

Ahmad R, Kumar R (2010) Adsorption studies of hazardous malachite green onto treated ginger waste. J Environ Manage 91(4):1032–1038. https://doi.org/10.1016/j.jenvman.2009.12.016

Ahmaruzzaman M (2011) Gupta VK (2011) Rice husk and its ash as low-cost adsorbents in water and wastewater treatment. Ind Eng Chem Res 50:13589–13613. https://doi.org/10.1021/ie201477c

Amin M, Ahmad M, Farooqi A, Hussain Q, Ahmad M, Al-Wabel M, Saleem H (2020) Arsenic release in contaminated soil amended with unmodified and modified biochars derived from sawdust and rice husk. J Soils Sediments 20:3358–3367

Arslana G, Tor A et al (2011) Removal of arsenate [As(V)] and arsenite [As(III)] from water by SWHR and BW-30 reverse osmosis Desalination, Volume 281:88–92. https://doi.org/10.1016/j.desal.2011.07.062

Asere TS, Stevens CV, Laing GD (2019) Use of (modified) natural adsorbents for arsenic remediation: a review. Sci Total Environ 676:706–720. https://doi.org/10.1016/j.scitotenv.2019.04.237

Asif Z, Chen Z (2017) Removal of arsenic from drinking water using rice husk. Appl Water Sci 7(3):1449–1458. https://doi.org/10.1007/s13201-015-0323-x

Askaruly K, Azat S, Sartova Z et al (2020) Obtaining and characterization of amorphous silica from rice husk. J Chem Technol 55(1):88–97

Ayoob S, Gupta AK, Bhagat PB (2007) Analysis of breakthrough developments and modeling of fixed bed adsorption system for As(V) removal from water by modified calcined bauxite (MCB). Sep Purif Technol 52(3):430–438. https://doi.org/10.1016/j.seppur.2006.05.021

Babazad Z, Kaveh F, Ebadi M et al (2021) Efficient removal of lead and arsenic using macromolecule-carbonized rice husks. Heliyon 7(3):e06631. https://doi.org/10.1016/j.heliyon.2021.e06631

Bansal M, Garg U, Singh D, Garg VK (2009) Removal of Cr(VI) from aqueous solutions using pre-consumer processing agricultural waste: a case study of rice husk. J Hazard Mater 162(1):312–320. https://doi.org/10.1016/j.jhazmat.2008.05.037

Baral SS, Das N, Ramulu TS et al (2009) Removal of Cr(VI) by Thermally activated weed Salvinia Cucullata in a fixed-bed column. J Hazard Mater 161(2–3):1427–1435. https://doi.org/10.1016/j.jhazmat.2008.04.127

Batur E, Baytar O, Kutluay S, Horoz S, Sahin O (2021) A comprehensive new study on the removal of Pb (II) from aqueous solution by sirnak coal-derived char. Environ Technol 42(3):505–520. https://doi.org/10.1080/09593330.2020.1811397

Baytar O et al (2021) Production of activated carbon from Elaeagnus angustifolia seeds using H3PO4 activator and methylene blue and malachite green adsorption. Int J Phytorem 23(7):693–703. https://doi.org/10.1080/15226514.2020.1849015

Bhakat PB, Gupta AK, Ayoob S (2007) Feasibility analysis of As(III) removal in a continuous flow fixed bed system by modified calcined bauxite (MCB). J Hazard Mater 139(2):286–292. https://doi.org/10.1016/j.jhazmat.2006.06.037

Bui TH, Pham VS, Thanh-Nho N, Trieu QA (2021) Removal of arsenic from water using a composite of iron–manganese oxide incorporated active rice husk silica. Clean Soil Air Water 49(4). https://doi.org/10.1002/clen.202000233

Byambaa E, Seon J, Kim TH et al (2021) Arsenic (V) removal by an adsorbent material derived from acid mine drainage sludge. Appl Sci 11:47. https://doi.org/10.3390/app11010047

Charola S, Yadav R, Das P et al (2018) Fixed-bed adsorption of Reactive Orange 84 dye onto activated carbon prepared from empty cotton flower agro-waste. Sustain Environ Res 28:298e308. https://doi.org/10.1016/j.serj.2018.09.003

Chen W, Parette R, Zou J et al (2007) Arsenic removal by iron-modified activated carbon. Water Res 41(9):1851–1858. https://doi.org/10.1016/j.watres.2007.01.052

Chowdhury ZZ, Hamid SBA, Zain SM (2015) Evaluating design parameters for breakthrough curve analysis and kinetics of fixed bed columns for Cu (II) cations using lignocellulosic wastes. BioResource 10(1):732–749

Daffalla SB, Mukhtar H, Shaharun MS (2012) Properties of activated carbon prepared from rice husk with chemical activation. Int J Glob Environ Issues 12(2–4):107–129. https://doi.org/10.1504/IJGENVI.2012.049375

Dang SV, Kawasaki J, Abella LC et al (2009) Removal of arsenic from simulated groundwater by adsorption using iron-modified rice husk carbon. J Water Environ Technol 7(2):43–56

Deshmukh P, Bhatt J, Peshwe D, Pathak S (2012) Determination of silica activity index and XRD, SEM and EDS studies of amorphous SiO2 extracted from rice husk ash. Trans Indian Inst Met 65(1):63–70. https://doi.org/10.1007/s12666-011-0071-z

Dotto GL, Santos JMND, Rosa R et al (2015) Fixed bed adsorption of Methylene Blue by ultrasonic surface modified chitin supported on sand. Chem Eng Res Des 100:302–310. https://doi.org/10.1016/j.cherd.2015.06.003

Ece MS, Kutluay S, Şahin O, Horoz S (2020) Development of novel Fe3O4/AC@SiO2@1,4-DAAQ magnetic nanoparticles with outstanding VOC removal capacity: characterization, optimization, reusability, kinetics, and equilibrium studies. Ind Eng Chem Res 59(48):21106–21123. https://doi.org/10.1021/acs.iecr.0c03883

El-Shafey EI (2007) Sorption of Cd(II) and Se(IV) from aqueous solution using modified rice husk. J Hazard Mater 147(1–2):546–555. https://doi.org/10.1016/j.jhazmat.2007.01.051

Fallah N, Taghizadeh M (2020) Continuous fixed-bed adsorption of Mo(VI) from aqueous solutions by Mo(VI)-IIP: breakthrough curves analysis and mathematical modeling. J Environ Chem Eng 8(5):104079. https://doi.org/10.1016/j.jece.2020.104079

Francisca FM, Carro Pérez ME (2014) Arsenic removal by coagulation-flocculation processes. Revista Internacional de Contaminacion Ambiental 30(2):177–190. https://www.researchgate.net/publication/298832835_Arsenic_removal_by_coagulation-flocculation_processes

Gilhotra V, Yadav R, Sugha A et al (2021) Electrochemical treatment of high strength chrome bathwater: a comparative study for best-operating conditions. Clean Eng Technol 2:100093. https://doi.org/10.1016/j.clet.2021.100093

Giri BS et al (2020) Adsorption of patent blue V from textile industry wastewater using Sterculia alata fruit shell biochar: evaluation of efficiency and mechanisms. Water 12(7). https://doi.org/10.3390/w12072017

Golberg S (2002) Competitive adsorption of arsenate and arsenite on oxides and clay minerals. Soil Sci Soc Am J 66:413–421

Golie WM, Upadhyayula S (2016) Continuous fixed-bed column study for the removal of nitrate from water using chitosan/alumina composite. J Water Process Eng 12:58–65. https://doi.org/10.1016/j.jwpe.2016.06.007

Goyal M, Bhagat M, Dhawan R (2009) Removal of mercury from water by fixed bed activated carbon columns. J Hazard Mater 171(1–3):1009–1015. https://doi.org/10.1016/j.jhazmat.2009.06.107

Han B, Runnells T, Zimbron JA (2002) Arsenic removal from drinking water by flocculation and microfiltration. Desalination 145(1):293–298. https://doi.org/10.1016/S0011-9164(02)00425-3

Han R, Ding D, Xu Y et al (2008) Use of rice husk for the adsorption of congo red from aqueous solution in column mode. Biores Technol 99(8):2938–2946. https://doi.org/10.1016/j.biortech.2007.06.027

Hummadi KK, Luo S, He S et al (2022) Adsorption of methylene blue dye from the aqueous solution via bio-adsorption in the inverse fluidized-bed adsorption column using the torrefied rice husk.

Chemosphere 287:131907. https://doi.org/10.1016/j.chemosphere.2021.131907

Hutchins R (1973) New method simplifies the design of activated carbon systems. Chem Eng 80(19):33–138

Islam MA et al (2017) Nanoporous activated carbon prepared from karanj (Pongamia pinnata) fruit hulls for methylene blue adsorption. J Taiwan Inst Chem Eng 74:96–104. https://doi.org/10.1016/j.jtice.2017.01.016

Islam A, Teo SH, Ahmed MT et al (2021) Novel micro-structured carbon-based adsorbents for notorious arsenic removal from wastewater. Chemosphere 272:129653. https://doi.org/10.1016/j.chemosphere.2021.129653

Jain M, Garg VK, Kadirvelu K (2013) Cadmium(II) sorption and desorption in a fixed bed column using sunflower waste carbon calcium-alginate beads. Biores Technol 129:242–248. https://doi.org/10.1016/j.biortech.2012.11.036

Jung K, Oh S, Bak H et al (2019) Adsorption of arsenic and lead onto stone powder and chitosan-coated stone powder. Processes 7(9):599. https://doi.org/10.3390/pr7090599

Kalderis D, Kotti MS, Mendez A, Gasco G (2014) Characterization of hydrochars produced by hydrothermal carbonization of rice husk. Solid Earth 5(1):477–483. https://doi.org/10.5194/se-5-477-2014

Khalil U, Shakoor MB, Ali S et al (2021) Selective removal of hexavalent chromium from wastewater by rice husk: kinetic, isotherm and spectroscopic investigation. Water 13:263. https://doi.org/10.3390/w13030263

Khan T, Wahap SABA, Chaudhuri (2012) Adsorption of arsenite from water by rice husk silica. Nat Env Poll Tech 11:229–233. https://neptjournal.com/upload-images/NL-38-9-(9)B-1861.pdf

Krishnani KK, Meng X, Christodoulatos C, Boddu VM (2008) Biosorption mechanism of nine different heavy metals onto biomatrix from rice husk. J Hazard Mater 153:1222–1234. https://doi.org/10.1016/j.jhazmat.2007.09.113

Kurian M (2021) Advanced oxidation processes and nanomaterials—a review. Clean Eng Technol 2:100090. https://doi.org/10.1016/j.clet.2021.100090

Kutluay S, Baytar O, Sahin O, Arran A (2020a) Optimization of process conditions for adsorption of methylene blue on formaldehyde-modified peanut shells using box-behnken experimental design and response surface methodology. Eur J Tech (EJT) 10(1):131–142. https://doi.org/10.36222/ejt.649205

Kutluay S, Ece MS, Sahin O (2020b) Synthesis of magnetic Fe3O4/AC nanoparticles and its application for the removal of gas-phase toluene by adsorption process. Int J Chem Technol 4(2):146–155. https://doi.org/10.32571/ijct.755732

Liao P, Zhan Z, Dai J et al (2013) Adsorption of tetracycline and chloramphenicol in aqueous solutions by bamboo charcoal: a batch and fixed-bed column study. Chem Eng J 228:496–505. https://doi.org/10.1016/j.cej.2013.04.118

Lin L, Qiu W, Wang D et al (2017) Arsenic removal in aqueous solution by a novel Fe-Mn modified biochar composite: characterization and mechanism. Ecotoxicol Environ Saf 144:5144–5521. https://doi.org/10.1016/j.ecoenv.2017.06.063

Liu X, Ao H, Xiong X et al (2012) Arsenic removal from water by iron-modified bamboo charcoal. Water Air Soil Pollut 223:1033–1044. https://doi.org/10.1016/j.heliyon.2019.e01577

Liu ST, Chen XG, Zhang AB et al (2014) Electromagnetic performance of rice husk ash. Bio Resources 9(2):2328–2340. https://doi.org/10.15376/biores.9.2.2328-2340

Lou J, Xu X, Gao Y et al (2016) Preparation of magnetic activated carbon from waste rice husk for the determination of tetracycline antibiotics in water samples. RSC Adv 113. https://doi.org/10.1039/C6RA24397E

Maher A, Sadeghi M, Moheb, (2014) Heavy metal elimination from drinking water using nanofiltration membrane technology and process optimization using response surface methodology.

Desalination 352:166–173. https://doi.org/10.1016/j.desal.2014.08.023

Maji SK, Pal A, Pal T (2008) Arsenic removal from real-life groundwater by adsorption on laterite soil. J Hazard Mater 150:811–820. https://doi.org/10.1016/j.jhazmat.2007.06.060

Maji SK, Kao YH, Guang-Sin CJ et al (2012) Fixed bed adsorption of As(III) on iron-oxide-coated natural rock (IOCNR) and application to real arsenic-bearing groundwater. Chem Eng J 203:285–293. https://doi.org/10.1016/j.cej.2012.07.033

Marzbali MH, Esmaieli M (2017) Fixed bed adsorption of tetracycline on a mesoporous activated carbon: experimental study and neuro-fuzzy modeling. J Appl Res Technol 15:454–463. https://doi.org/10.1016/j.jart.2017.05.003

Masoud MS, El-Saraf WM, Abdel - Halim AM et al (2016) Rice husk and activated carbon for waste water treatment of El-Mex Bay, Alexandria Coast, Egypt. Arab J Chem 9: S1590-S1596. https://doi.org/10.1016/j.arabjc.2012.04.028

McKay G (1979) Basic dye adsorption on activated carbon. Water Air Soil Pollut 12:307–317

Mohamed RM, Mkhalid IA, Barakat MA (2015) Rice husk ash as a renewable source for the production of zeolite NaY and its characterization. Arab J Chem 8(1):48–53. https://doi.org/10.1016/j.arabjc.2012.12.013

Mohan S, Singh DK, Kumar V et al (2017) Modelling of fixed bed column containing graphene oxide decorated by MgO nanocubes as adsorbent for Lead(II) removal from water. J Water Process Eng 17:216–228. https://doi.org/10.1016/j.jwpe.2017.03.009

Mohan D, Markandeya DS et al (2019) Adsorption of arsenic using low cost adsorbents: guava leaf biomass, mango bark and bagasse. Curr Sci 117(4):649–661

Mukherjee S, Thakur AK, Goswami R et al (2021) Efficacy of agricultural waste derived biochar for arsenic removal: tackling water quality in the Indo-Gangetic plain. J Environ Manage 281:111814. https://doi.org/10.1016/j.jenvman.2020.111814

Nguyen N, Nguyen D, Pham D et al (2017) New oligochitosan-nanosilica hybrid materials: preparation and application on chili plants for resistance to anthracnose disease and growth enhancement. Polym J 49:861–869. https://doi.org/10.1038/pj.2017.58

Nicomel NR, Leus K, Folens K et al (2015) Technologies for arsenic removal from water: current status and future perspectives. Int J Environ Res Public Health 13(1):1–24. https://doi.org/10.3390/ijerph13010062

Noel WC, Chen ZL, Bacharou T (2021) Arsenic removal from water by nanofiltration membrane: potentials and limitations. Water Pract Technol 16:1–3. https://doi.org/10.2166/wpt.2021.018

Nurul AM, Satoshi K, Taichi K et al (2006) Removal of arsenic in aqueous solutions by adsorption onto waste rice husk". Ind Eng Chem Res 45(24):8105–8110. https://doi.org/10.1021/ie060344j

Patel H, Vashi RT (2015) characterization and column adsorptive treatment for cod and color removal using activated neem leaf powder from textile wastewater. J Urban Environ Eng 9(1):45–53. https://doi.org/10.4090/juee.2015.v9n1.045053

Pehlivan E, Tran TH, Ouédraogo WKI et al (2013) Removal of As(V) from aqueous solutions by iron coated rice husk. Fuel Process Technol 106:511–551. https://doi.org/10.1016/j.fuproc.2012.09.021

Pholosi A, Naidoo EB, Ofomaja AE (2020) Batch and continuous flow studies of Cr(VI) adsorption from synthetic and real wastewater by magnetic pine cone composite. Chem Eng Res Des 153:806–818. https://doi.org/10.1016/j.cherd.2019.11.004

Rasouli A, Bafkar A, Chaghakabooli Z (2020) Kinetic and equilibrium studies of adsorptive removal of sodium-ion onto wheat straw and rice husk wastes. Central Asian Journal of Environmental Science and Technology Innovatopn 6:310–329. https://doi.org/10.22034/CAJESTI.2020.06.04

Roy P, Mondal NK, Bhattacharya S et al (2013) Removal of arsenic(III) and arsenic(V) on chemically modified low-cost adsorbent: batch and column operations. Appl Water Sci 3:293–309. https://doi.org/10.1007/s13201-013-0082-5

Sahin O, Kutluay S, Horoz S, Ece MS (2021) Fabrication and characterization of 3,4-diaminobenzophenone-functionalized magnetic nanoadsorbent with enhanced VOC adsorption and desorption capacity. Environ Sci Pollut Res 28:5231–5253. https://doi.org/10.1007/s11356-020-10885-y

Samad A, Fukumoto T, Dabwan AHA et al (2016) Enhanced removal of arsenite from ground water by adsorption onto heat-treated rice husk. Open J Inorg Non Met Mater 6(3):18–23. https://doi.org/10.4236/ojinm.2016.63004

Senthilkumar R, Prasad DMR, Govindarajan L (2020) Synthesis of green marine algal-based biochar for remediation of arsenic(V) from contaminated waters in batch and column mode of operation. Int J Phytoremediation 22(3):279–286. https://doi.org/10.1080/15226514.2019.1658710

Shahlae M, Pourhossein A (2014) Determination of arsenic in drinking water samples by electrothermal atomic absorption spectrometry after preconcentration using the biomass of Aspergillus niger loaded on activated charcoal. J Chem 2014: Article ID 912619. https://doi.org/10.1155/2014/912619

Shen ZX (1997) Use of arsenic trioxide (AS2O3) in the treatment of acute promyelocytic leukemia (AFL): II. Clinical efficacy and pharmacokinetics in relapsed patients. Blood 89(9): 3354–60. https://pubmed.ncbi.nlm.nih.gov/9129042/

Shipley HJ, Yean S, Kan AT, Tomson MB (2009) Adsorption of arsenic to magnetite nanoparticles: effect of particle concentration, pH, ionic strength, and temperature. Environ Toxicol Chem 28(3):509–515. https://doi.org/10.1897/08-155.1

Siddiqa A, Shahida S, Qaisar S (2019) Titanium-based nanocomposite materials for arsenic removal from water: a review Sobia Ashraf a. Heliyon 5(5):E01577. https://doi.org/10.1016/j.heliyon.2019.e01577

Siddiqui SI, Chaudhry SA (2017) Removal of arsenic from water through adsorption onto metal oxide-coated material. Materials Research Foundations In Applications of Adsorption and Ion Exchange Chromatography in Waste Water Treatment 15pp:227–276. https://doi.org/10.21741/9781945291333-9

Singh ST, Pant KK (2006) Experimental and modeling studies on fixed bed adsorption of As(III) ions from aqueous solution. Sep Purif Technol 48(3):288–296. https://doi.org/10.1016/j.seppur.2005.07.035

Song ST, Hau YF, Saman N et al (2016) Process analysis of mercury adsorption onto chemically modified rice straw in a fixed-bed adsorber. J Environ Chem Eng 4(2):1685–1697. https://doi.org/10.1016/j.jece.2016.02.033

Srivastava VC, Prasad B, Mishra IM et al (2008) Prediction of breakthrough curves for sorptive removal of phenol by bagasse fly ash packed bed. Ind Eng Chem Res 47(5):1603–1613. https://doi.org/10.1021/ie0708475

Treybal RE (1981) Mass Transfer Operations. McGraw-Hill chemical engineering series; McGraw-Hill class ic textbook ,reissue series, 3rd Edn/Format: Print book : English. Publisher: New York : McGraw Hill Book Company Inc., ©1981

Yan G, Viraraghavan T, Chen M (2001) A new model for heavy metal removal in a biosorption column. Adsorpt Sci Technol 19(1):25–43. https://doi.org/10.1260/0263617011493953

Yu W, Liang Q, Yin Y et al (2021) Adsorption of arsenite by core–shell K-OMS-2@UiO-66 microspheres: performance and mechanism. New J Chem 34:2020

Zaw M, Emett MT (2002) Arsenic removal from water using advanced oxidation processes. Toxicol Lett 133(1):113–118. https://doi.org/10.1016/S0378-4274(02)00081-4

Zhang T, Zhuo C, Lu L, Jin Y et al (2017) Removal of Cr(VI) by modified and immobilized Auricularia Auricula spent substrate in a fixed-bed column. Ecol Eng 99:358–365. https://doi.org/10.1016/j.ecoleng.2016.11.070

Zhao Y, Huang M, Wu W et al (2009) Synthesis of the cotton cellulose based Fe(III)-loaded adsorbent for arsenic(V) removal from drinking water. Desalination 249(3):1006–1011. https://doi.org/10.1016/j.desal.2009.09.015